Soft Matter

PAPER

View Article Online
View Journal | View Issue

Cite this: *Soft Matter*, 2016, **12**, 3184

The microscopic structure of mono-disperse granular heaps and sediments of particles on inclined surfaces

Nikola Topic,[a] Fabian M. Schaller,[b] Gerd E. Schröder-Turk[bc] and Thorsten Pöschel*[a]

Received 28th July 2015,
Accepted 3rd February 2016

DOI: 10.1039/c5sm03114a

www.rsc.org/softmatter

Granular heaps of particles created by deposition of mono-disperse particles raining from an extended source of finite size are characterized by a non-homogeneous field of density. It was speculated that this inhomogeneity is due to the transient shape of the sediment during the process of construction of the heap, thus reflecting the history of the creation of the heap. By comparison of structural characteristics of the heap with sediments created on top of inclined planes exploiting the method of Minkowski tensors, we provide further evidence to support this hypothesis. Moreover, for the case of sediments generated by homogeneous rain on surfaces, we provide relationships between the inclination of the surface and the Minkowski measures characterizing the isotropy of local particle environments.

1 Introduction

Structural properties of mono-disperse packings belong to the most intensively investigated systems, starting with Kepler's conjecture of 1611,[1] concerning the maximal packing density of an assembly of equal spheres. Packings of hard particles have been the focus of a large number of studies, and a large variety of phenomena were described in the literature, see *e.g.* ref. 2–5 and many references therein.

The structural properties of packings are intimately related to certain macroscopic properties of granular matter such as sound propagation,[6] thermal conductivity,[7] permeability,[8] reactivity,[9] tensile strength,[9] dilation[10] and others. Of particular recent interest is the relationship of the microstructure of packings in the jammed state and the process of jamming in granular dynamics, *e.g.* ref. 5 and 11–17.

The microscopic structure of a sediment and, thus, its macroscopic characteristics depend, of course, on geometric factors such as sizes, size distribution and shapes of the particles. But, moreover, they depend on mechanical factors,[18,19] that is, the conditions under which the packing is formed. That is, the macroscopic characteristics of a granular packing depend on the history of the packing process, see *e.g.* ref. 20.

A prominent example where the history of the packing process leaves its fingerprint on the microstructure of the sediment is a monodisperse heap of spheres created on a horizontal plane due to a homogeneous rain of particles from a circular area source with steepest descent relaxation.[21] During the creation process, the particles are dropped sequentially from random positions in the source area and follow the steepest descent of energy in the potential landscape formed by previously deposited particles until the particle reaches a local minimum or touches the bottom plane, where it is immobilized. The described paradigm specifies the protocol of the dynamics employed in the present article. The described dynamics can be formulated by an efficient event-driven algorithm[22,23] which allows for the simulation of very large sediments exceeding 10^7 particles. Initially due to the homogeneous rain of particles, only the region under the source is covered by sediment. As the heap grows, the sediment assumes the shape of a frustum of a cone with a horizontal top surface and finally it turns into a cone, see Fig. 1 and ref. 24 for a detailed description of the process.

By analysis of the local packing density and the field of contact numbers it was found recently that such a heap has a complex internal structure.[24] It was argued that this structure is due to the different types of motion of particles during the process of sedimentation: type (a) – outside the dropping zone (the dropping zone is defined as the volume below the source area), only such local minima can become occupied by a particle which are terminal points of a uninterrupted path of steepest descent, starting at some point in the source area. Type (b): inside the source region all local minima may become populated, either by steepest descent motion or by randomly directly dropping into the basin of attraction of the local minimum. Thus, there are local minima which can be populated by the process of type (b) but not of type (a)

[a] *Institute for Multiscale Simulation, Friedrich-Alexander-Universität Erlangen-Nürnberg, Erlangen, Germany. E-mail: thorsten.poeschel@fau.de*
[b] *Theoretische Physik I, Friedrich-Alexander-Universität Erlangen-Nürnberg, Erlangen, Germany*
[c] *Murdoch University, School of Engineering and IT, Mathematics and Statistics, Murdoch, Western Australia 6150, Australia*

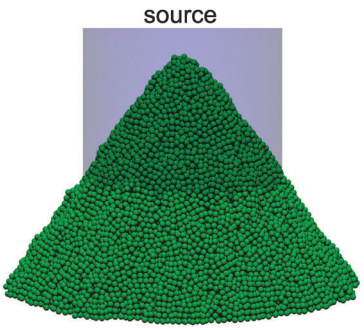

Fig. 1 Heap created by sequentially dropping particles from a circular area source. The width of the source is shaded gray.

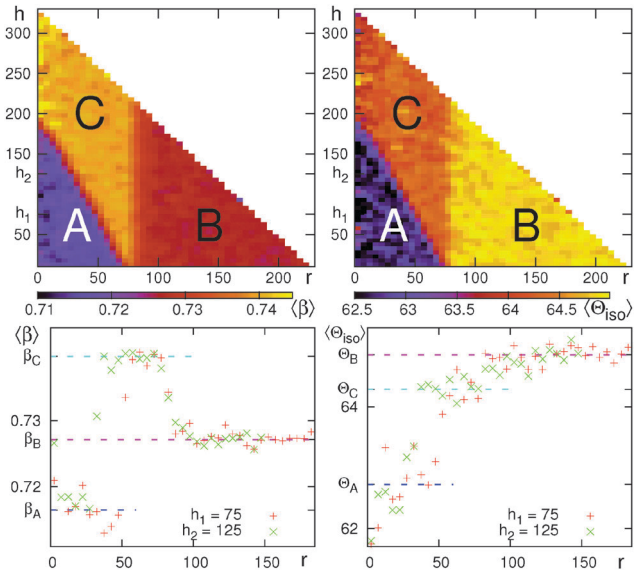

Fig. 2 (top) Both quantities are averaged with respect to the cylinder symmetry of the system. The field of isotropy (left) and the angle of isotropy (right) for a heap of 2.5×10^7 particles. The bin widths are $\Delta h = \Delta r = 5$. Note that bins with larger r values include more particles. Well separated zones of $\langle\beta\rangle(r,h)$ and $\langle\theta_{\mathrm{iso}}\rangle(r,h)$ are identical to zones of density described in ref. 24. (bottom) $\langle\beta\rangle(r)$ and $\langle\theta_{\mathrm{iso}}\rangle(r)$ profiles for two different horizontal cuts with $h_1 = 75$ and $h_2 = 125$. All units are in particle diameters.

leading to a slightly higher density in regions where historically the heap was built due to type (b). Consequently, these mechanisms result in 3 regions of different densities: region (B) outside the dropping zone (type (a)), region (A) under the dropping zone where historically the sediment was horizontal (type (b)), and region (C) under the dropping zone where historically the surface was inclined by the angle of repose, see Fig. 2.

2 Characterization of the structure of the sediment

In this paper, by means of Minkowski tensors, we quantify the micro-structural properties of the heap sediment. By comparison with sediments built on an inclined plane we will show that because of the process of construction, regions A and C are fundamentally different from region B. We will demonstrate that Minkowski tensors can be used to reveal the history of the formation of a sediment by analyzing its final structure.

A recently developed way to quantify the structure of granular packings are Minkowski tensors.[25,26] Minkowski tensors are a generalization of the Minkowski functionals, which are the volume, the surface area, the mean curvature integrated over the surface and the Euler-Poincaré index of a body. Every additive tensorial functional of a body can be written as a finite sum of the Minkowski tensors.[27] For three-dimensional bodies, there are 10 Minkowski tensors of rank two. A detailed explanation is given in ref. 28. Here we apply these tensors to the particles Voronoï cells. We focus on the volume moment tensor of rank two

$$\mathbf{W}_0^{20} \equiv \int_K \vec{r} \otimes \vec{r}\,\mathrm{d}V, \tag{1}$$

where the integral is performed over the volume V of the body K (the Voronoï cell) and the tensor product is defined as $\left(\vec{a} \otimes \vec{b}\right)_{ij} \equiv \frac{1}{2}(a_i b_j + a_j b_i)$. Note that $\mathbf{W}_0^{20}$ is related to the tensor of inertia of the body.[29] It depends on the choosen origin, which is in our case the center of the containing particle of the cell, see below.

In order to characterize the anisotropy of a packing, first we compute its Voronoï tessellation. Then, for each Voronoï cell the tensor $\mathbf{W}_0^{20}$ is calculated with respect to the center of the sphere to which the Voronoï volume corresponds. We consider two measures derived from the tensors $\mathbf{W}_0^{20}$, namely the isotropy, defined as the ratio

$$\beta \equiv \frac{|\mu_{\min}|}{|\mu_{\max}|} \tag{2}$$

of the smallest and the largest eigenvalue of $\mathbf{W}_0^{20}$ (note that the eigenvalues are positive). β has theoretical values between 0 (the limit of an extremly anisotropic cell) and 1 (isotropic cell), although in random sphere packs β varies from approximately 0.67 to 0.80.[25,26] The second quantity is the angle of isotropy, θ_{iso}, defined as the angle between the positive direction of the vertical z axis (the direction of gravity) and the eigenvector corresponding to the largest eigenvalue of the tensor $\mathbf{W}_{20}^0$. θ_{iso} has theoretical values between 0° and 90°. A packing fraction (or density), ρ, corresponding to the particle and its Voronoï cell is calculated by dividing the particle's volume by the volume of the cell.

For the characterization of a heap created by dropping 2.5×10^7 monodisperse particles homogeneously from a circular source with diameter $S = 80$ measured in units of particle diameters, we use cylindrical coordinates. Both quantities, β and θ_{iso}, are thus fields of the cylindrical coordinates. Due to the symmetry in the horizontal coordinates, we average over the angular coordinate such that $\langle\beta\rangle(r,h)$ and $\langle\theta_{\mathrm{iso}}\rangle(r,h)$ are the fields of isotropy and the angle of isotropy averaged over all particles whose centers are located in small intervals of height, h, and the distance from the vertical symmetry axis, r, see Fig. 2.

Table 1 Mean values and standard deviations of ρ, β and θ_{iso} of the different zones

Zone	$\langle\rho\rangle$	$\sigma(\rho)$	$\langle\beta\rangle$	$\sigma(\beta)$	$\langle\theta_{iso}\rangle$ (°)	$\sigma(\theta_{iso})$ (°)
A	0.5813	0.0325	0.717	0.086	62.72	20.10
B	0.5832	0.0319	0.727	0.088	64.85	19.58
C	0.5874	0.0296	0.740	0.082	64.29	19.61

The field of packing fraction $\langle\rho\rangle(r,h)$ was calculated in an analogous way.

As Fig. 2 clearly shows, the heap reveals three well separated zones for both isotropy characteristics, β and θ_{iso}, denoted A, B, and C. These zones are identical to the zones of different densities identified in ref. 24 for the same system. A fourth zone (D) described in ref. 24 is not discussed here since its volume is rather small and unlike the other zones it does not scale with the volume of the heap which is problematic for averaging and results in large fluctuations. Zone averages are defined as *e.g.* $\beta_A = \langle\beta\rangle_{sphere\in A}$, see Table 1. The width of the distributions within the zones is given by *e.g.* $\sigma(\beta)$. As shown in Table 1, the values of the angle of isotropy θ_{iso} are widely distributed but, however, statistical averages of this parameter are able to point out significant structural differences in the zones.

In the following, we consider the relation of $\langle\beta\rangle$ and $\langle\theta_{iso}\rangle$ as a function of packing density.

3 Isotropy and angle of isotropy as a function of density

When a heap is deposited from particle rain due to a circular homogeneous area source, it initially grows with a horizontal top surface, *i.e.* it is frustum of a cone whose inclination is the angle of repose, α_{rep}, which for our model fluctuates in the range $\alpha_{rep} \approx 54°$, regardless of the size of the source, S,[30] being the only parameter of the system. Consequently, the surface of the heap assumes only the two extremal values of inclination, $\alpha = 0°$ in the region under the source and $\alpha = \alpha_{rep}$, corresponding to low and high values of density, respectively.

In order to study the relationship between surface inclination, α, and density, ρ, in more detail, we performed simulations where 10^6 particles of diameter 1 are deposited on an inclined plane. The projection of the plane to horizontal is of size $L \times L = 100^2$ and it is

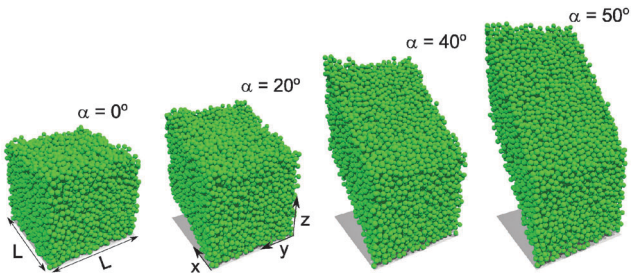

Fig. 3 Sediments due to a homogeneous rain of 8000 particles on inclined planes. The horizontal plane is shown in gray.

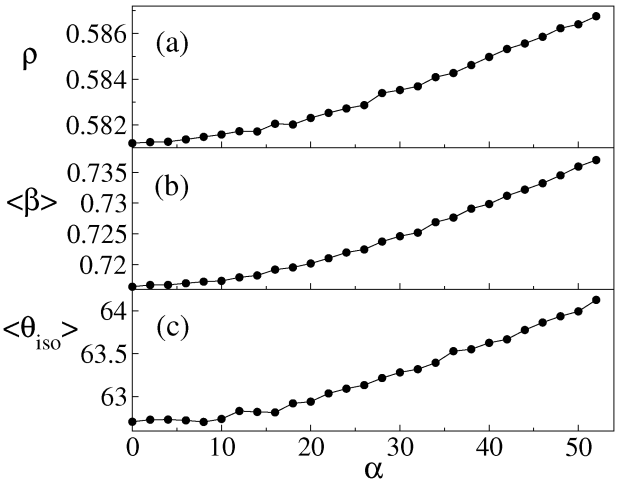

Fig. 4 Average packing fraction (a), isotropy (b), and the angle of isotropy (c) of a sediment of particles deposited on an inclined plane as a function of the angle of inclination, α.

inclined by $\alpha = 0°\ldots\alpha_{rep}$ with periodic boundary conditions in the lateral direction, see Fig. 3.

Values of packing fraction, ρ, isotropy, β, and angle of isotropy, θ_{iso}, are averaged over particles inside the packing. We neglect particles closer than 10 diameters to the incline to avoid the influence of ordered structures imposed by the vicinity of the flat wall as well as particles closer than 10 diameters to the top of the packing. Fig. 4a shows the packing fraction as a function of inclination. The increase of packing fraction with the tilt has been noted before in ref. 31. Obviously, the range of inclination is limited by the angle of repose, α_{rep}, since for steeper tilt the particles would not reach a stable position. In our simulations we found reliable results for $\alpha \lesssim 52°$. Note that this value is somewhat smaller than α_{rep} due to the fact that on a finite surface with periodic boundary conditions there may occasionally exist continuous paths of steepest descent even for inclinations less than the angle of repose, such that the system would not find a stable position.

The isotropy as a function of the inclination is an increasing function as well which at first glance may appear counter-intuitive, Fig. 4b. The result becomes clear when we note that the only source of anisotropy is the direction of gravity. For $\alpha = 0$, the surface of the sediment is perpendicular to gravity such that one direction is preferred over the others. For larger inclination, this effect is much less pronounced, leading to larger values of the isotropy characteristics. Finally, the angle of isotropy, Fig. 4c, as a function of inclination angle shows a similar behavior as isotropy.

For a quantitative comparison of the packings we plot the isotropy characteristics as a function of density, $\langle\beta\rangle(\rho)$ and $\langle\theta_{iso}\rangle(\rho)$, Fig. 5. For sediments created on inclines (bullets), both functions are approximately linear in the entire range of density corresponding to the interval of inclination, $0 \leq \alpha \lesssim \alpha_{rep}$. Looking to the data points for the heap, we find that the points for areas A and C agree with the data for the tilted plane. This is consistent with the inclination of the historical surface

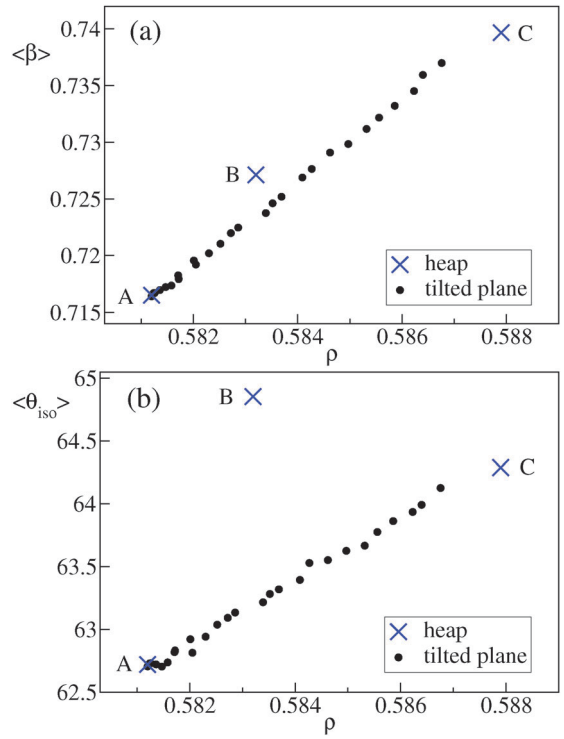

Fig. 5 Isotropy (a) and angle of isotropy (b) as a function of the packing fraction for both types of sediments, heap and the inclined plane. For the case of the heap, the areas A, B, and C were evaluated separately.

of the heap during construction, $\alpha = 0$ in region A and $\alpha = \alpha_{rep}$ in region C. Thus, the sediments on the incline and in the heap regions A and C may be considered as packings of the same type.

In contrast, the data for area B are distinctly different to the other data, indicating a distinct structure which can be understood from the history of the heap: stable sites on the heap's surface that are not below the source of particles (region B) can only be reached by particles travelling along paths of steepest descent. Sites which are not terminal points of steepest descent paths cannot be populated. In contrast, stable sites under the source (regions A and C) can be occupied by particles traveling along steepest descent paths and by particles dropping from the source and landing in the vicinity (in the basin of attraction) of the stable site. This way, stable sites can be populated which are unaccessible by steepest descent motion. The different mechanism of growth, thus, causes differences in the microstructure of packings. Our analysis shows that Minkowski tensors are suitable to identify such subtle differences in growth mechanisms which indeed cause differences of the structure.

4 Conclusion

We have characterized sediments of monodisperse particles created by random deposition and steepest descent relaxation for two different cases: (a) particles raining from a homogeneous circular area source to a horizontal plane forming a conical heap and (b) sedimentation from a homogeneous rain onto a tilted plane with periodic lateral boundary conditions.

The packings were characterized using measures derived from Minkowski tensors of Voronoï cells corresponding to particles in the packing, namely the isotropy, β, and the angle of isotropy, θ_{iso}. We found that regions of the packing of the heap below the source of particles reveal the same structure as packings due to deposition of particles onto a tilted plane but are structurally different from packings generated outside the source region.

Consequently, based on Minkowski tensors we can identify the origin of different structures of sand heaps generated by particles raining from an extended source.[24] Functional dependences $\langle\beta\rangle(\rho)$ and $\langle\theta_{iso}\rangle(\rho)$, of the type shown in Fig. 5, may be applied to infer information about the history of a packing only based on the structure of the sediment, even when the process of its formation is not known.

In granular materials, different formation mechanisms can lead to relatively subtle structural differences in the resulting packing, which in turn affect its physical properties. Our results highlight the Minkowski tensor approach as a robust quantitative method to detect subtle but important structural differences. This is particularly relevant for systems, such as the one investigated here, where structural differences are only evident in averaged quantities, with large spatial fluctuations and broad distributions of the quantities themselves.

The investigated sediments result from a sequential random deposition with the steepest relaxation model as specified in Section 1. We wish to point out that this model and the corresponding dynamics is not a universal simulation method for granular matter dynamics for two reasons: (a) the particles are sedimented sequentially, that is, at any time only one particle is in motion, and (b) once a particle found its stable position it is immobilized and cannot leave this position under the action of later sedimented particles. This specific dynamics does, *e.g.*, not allow for steady flow or avalanches. However, under certain conditions this model for the dynamics may be appropriate, for instance, in viscous fluids when we can neglect inertia of the particles or in the case of adhesive particles when acceleration due to gravity can be neglected and the particles perform a creeping motion. For a full discussion of the properties of the model see ref. 30. Insofar, the results presented here may be specific for this type of dynamics and their possible generalization was not investigated. Clearly, a full size DEM or molecular dynamics investigation of the systems considered here, including the necessary repetition for averaging is certainly not feasible, at the present time.

Acknowledgements

We acknowledge funding by the German Science Foundation (DFG) through grant PO 472/22, the research group "Geometry and Physics of Spatial Random Systems" under grant SCHR-1148/3-2, and the Cluster of Excellence "Engineering of Advanced Materials".

References

1 J. Kepler, *Joannis Kepleri S. C. Maiest. Mathematici Strena Seu De Nive Sexangula*, Gottfried Tambach, Frankfurt, 1611.

2 T. Aste and D. Weaire, *The Pursuit of Perfect Packing*, Institute of Physics, London, 2000.
3 H. M. Jaeger, S. R. Nagel and R. P. Behringer, *Rev. Mod. Phys.*, 1996, **68**, 1259–1273.
4 J. Picka, *Stat. Surv.*, 2012, **6**, 74–112.
5 S. Torquato and F. H. Stillinger, *Rev. Mod. Phys.*, 2010, **82**, 2633–2672.
6 G. Cascante and J. Santamarina, *J. Geotech. Eng.*, 1996, **122**, 831–839.
7 J. Reimann, R. A. Pieritz and R. Rolli, *Fusion Eng. Des.*, 2006, **81**, 653–658.
8 R. P. Dias, C. S. Fernandes, M. Mota, J. A. Teixeira and A. Yelshin, *Int. J. Heat Mass Transfer*, 2007, **50**, 1295–1301.
9 L. Y. Yi, K. J. Dong, R. P. Zou and A. B. Yu, *Ind. Eng. Chem. Res.*, 2011, **50**, 8773–8785.
10 A. J. Kabla and T. J. Senden, *Phys. Rev. Lett.*, 2009, **102**, 228301.
11 P. Wang, C. Song, Y. Jin, K. Wang and H. A. Makse, *J. Stat. Mech.: Theory Exp.*, 2010, P12005.
12 C. Song, P. Wang and H. A. Makse, *Nature*, 2008, **453**, 629–632.
13 F. Lechenault, F. da Cruz, O. Dauchot and E. Bertin, *J. Stat. Mech.: Theory Exp.*, 2006, P07009.
14 J. Brujić, C. Song, P. Wang, C. Briscoe, G. Marty and H. A. Makse, *Phys. Rev. Lett.*, 2007, **98**, 248001.
15 M. Clusel, E. I. Corwin, A. O. N. Siemens and J. Brujić, *Nature*, 2009, **460**, 611–615.
16 T. Aste, *Phys. Rev. Lett.*, 2006, **96**, 018002.
17 K. J. Dong, R. Y. Yang, R. P. Zou, X. Z. An and A. B. Yu, *Europhys. Lett.*, 2009, **86**, 46003.
18 W. A. Gray, *The Packing of Solid Particles*, Chapman and Hall, London, 1968.
19 J. Dodds and H. Kuno, *Nature*, 1977, **266**, 614–615.
20 M. Tixier, O. Pitois and P. Mills, *Eur. Phys. J. E: Soft Matter Biol. Phys.*, 2004, **14**, 241–247.
21 W. M. Visscher and M. Bolsterli, *Nature*, 1972, 504–507.
22 W. S. Jodrey and E. M. Tory, *Simulations*, 1979, **32**, 1–12.
23 T. Pöschel and T. Schwager, *Computational Granular Dynamics: Models and Algorithms*, Springer, Berlin, Heidelberg, New York, 2005.
24 N. Topic, J. A. C. Gallas and T. Pöschel, *Phys. Rev. Lett.*, 2012, **109**, 128001.
25 G. E. Schröder-Turk, W. Mickel, M. Schröter, G. W. Delaney, M. Saadatfar, T. J. Senden, K. Mecke and T. Aste, *Europhys. Lett.*, 2010, **90**, 34001.
26 F. Schaller, S. Kapfer, J. Hilton, P. Cleary, K. Mecke, C. De Michele, T. Schilling, M. Saadatfar, M. Schröter, G. Delaney and G. Schröder-Turk, *Europhys. Lett.*, 2015, **111**, 24002.
27 S. Alesker, *Geom. Dedicata*, 1999, **74**, 241–248.
28 G. E. Schröder-Turk, W. Mickel, S. C. Kapfer, F. M. Schaller, B. Breidenbach, D. Hug and K. Mecke, *New J. Phys.*, 2013, **15**, 083028.
29 G. E. Schröder-Turk, W. Mickel, S. C. Kapfer, M. A. Klatt, F. M. Schaller, M. J. F. Hoffmann, N. Kleppmann, P. Armstrong, A. Inayat, D. Hug, M. Reichelsdorfer, W. Peukert, W. Schwieger and K. Mecke, *Adv. Mater.*, 2011, **23**, 2535–2553.
30 N. Topic, J. A. C. Gallas and T. Pöschel, *Philos. Mag.*, 2013, **93**, 4090–4107.
31 A. Higgins, *J. Phys. A: Math. Gen.*, 1996, **29**, 2373–2377.

